Electronic Journal of Biotechnology 68 (2024) 67–80

Contents lists available at ScienceDirect

Electronic Journal of Biotechnology

journal homepage: www.elsevier.com/locate/ejbt

Research article

In silico and *in vitro* assessment of the anti-β-amyloid aggregation and anti-cholinesterase activities of *Ptaeroxylon obliquum* and *Bauhinia bowkeri* extracts ☆

Michael C. Ojo [a,*], Rebamang A. Mosa [b], Foluso O. Osunsanmi [a], Neerish Revaprasadu [c], Andy R. Opoku [a]

[a] Department of Biochemistry and Microbiology, University of Zululand, Private Bag X1001, KwaDlangezwa 3886, South Africa
[b] Biochemistry, Genetics and Microbiology Department, Biochemistry Division, Faculty of Natural and Agricultural Science, University of Pretoria, Hatfield, South Africa
[c] Department of Chemistry, University of Zululand, Private Bag X1001, KwaDlangezwa 3886, South Africa

GRAPHICAL ABSTRACT

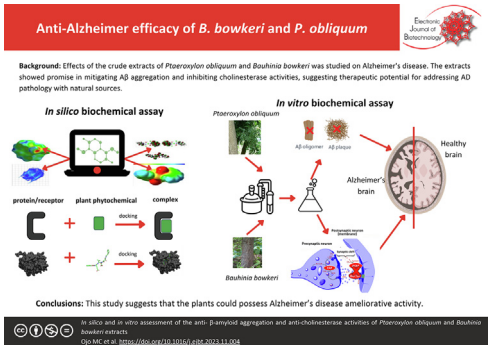

ARTICLE INFO

Article history:
Received 29 June 2023
Accepted 24 November 2023
Available online 16 December 2023

Keywords:
Acetylcholinesterase
Alzheimer's disease
Anti-aggregation
β-amyloid (Aβ)
Bauhinia bowkeri
β-secretase
Butyrylcholinesterase
Dementia
Phytochemicals
Ptaeroxylon obliquum

ABSTRACT

Background: Alzheimer's disease (AD) is the most common form of dementia and dementia constitutes the fifth leading cause of mortality across the globe. Available treatment modalities and drugs have abysmally failed to curtail AD. This study evaluated the mitigation of Aβ aggregation and anti-cholinesterase activities with the crude extracts of *Ptaeroxylon obliquum* and *Bauhinia bowkeri*. Computational studies of the most abundant phytochemicals from the crude extracts of both plants with proteins were investigated. The phytochemical composition of the different crude extracts (hexane, DCM, and ethanol) of the plants were analyzed with FTIR and GC-MS. The inhibitory potential of the extracts on BACE-1 and cholinesterase activities was determined with both computational molecular docking studies and *in vitro* enzyme assays. Their anti-aggregation properties were confirmed with Thioflavin-T assay and TEM.
Results: The *in silico* studies revealed that though thunbergol and cyclotetradecatriene (the major constituents of the extracts) inhibited all the proteins, the latter exhibited the best inhibitory potential. The *in vitro* results showed that while the dichloromethane (DCM) extract of *P. obliquum* had the highest butyrylcholinesterase (BuChE) inhibitory activity (1.77 μg/ml), the hexane and ethanol extract of *B. bowkeri* exhibited the highest β-site amyloid precursor cleaving enzymes-1 (BACE-1) (30.4 μg/ml) and

Abbreviations: Aβ, Beta amyloid; AChE, Acetylcholinesterase; AD, Alzheimer's disease; APOE, Apolipoprotein E; ARIA, Amyloid related imaging abnormalities; BACE-1, Beta site amyloid precursor protein cleaving enzymes 1; BuChE, Butyrylcholinesterase; FAD, Familial Alzheimer's disease; FTIR, Fourier transform infrared; GC-MS, Gas Column Mass spectroscopy; NMDA, N-methyl-D-aspartate; SAD, Sporadic Alzheimer's disease; TEM, Transmission Electron Microscope; ThT, Thioflavin T.

☆ Audio abstract available in Supplementary material.

Peer review under responsibility of Pontificia Universidad Católica de Valparaíso.

* Corresponding author.
E-mail address: mikekonyegwachie2015@gmail.com (M.C. Ojo).

https://doi.org/10.1016/j.ejbt.2023.11.004

acetylcholinesterase (AChE) (58.11 μg/ml) inhibitory efficacy, respectively. The ethanol extract (160 μg/ml) of *B. bowkeri* had the most efficacious anti-aggregation activity.
Conclusions: This study suggests that the plants could possess neuroprotective effects and could also be sources of anti-AD novel drugs.
How to cite: Ojo MC, Mosa RA, Osunsanmi FO, et al. *In silico* and *in vitro* assessment of the anti-β-amyloid aggregation and anti-cholinesterase activities of *Ptaeroxylon obliquum* and *Bauhinia bowkeri* extracts. Electron J Biotechnol 2024;68. https://doi.org/10.1016/j.ejbt.2023.11.004.

1. Introduction

The study looks at the *in silico* and *in vitro* assessment of the anti-β-amyloid aggregation and anti-cholinesterase activities of *Ptaeroxylon obliquum* and *Bauhinia bowkeri* extracts. Alzheimer's disease (AD) is a progressive brain change that is associated with cognitive decline, and behavioral and language impairment [1,2]. Alzheimer's disease (AD) referred to mainly disease of the elderly, is the commonest form of dementia and according to its etiology, can be classified into familial or early-onset AD (FAD) and sporadic also known as late-onset AD (SAD). Familial Alzheimer's disease, associated with genetic variations of the β-amyloid precursor proteins (APP), presenilins 1 and 2 (sub-units of γ-secretase), is responsible for few AD cases, while sporadic AD accounts predominantly for most people with AD.

Though AD has a genetic undertone specifically, the APOE ε4 lipoprotein, it is multifaceted [2,3,4,5]. Nevertheless, age is regarded as the major causative factor of AD [6]. Alzheimer's disease affects about 58 million of people globally [7] and projections made by the Alzheimer's disease facts and figures released in 2023 state that in the United States of America alone, about 13.8 million people aged 65 and above will suffer from AD by the year 2060 [8]. The histopathological epicenter of Alzheimer's disease is the senile plaques composed of β-amyloid and the hyperphosphorylated microtubule-associated tau-proteins organized into neurofibrillary tangles [4,9,10,11].

Sequential breakdown of the amyloid precursor protein (APP)- a single transmembrane found on the neuronal membrane that contributes to neuronal growth and repair, by the β-site amyloid precursor protein cleaving enzymes (BACE-1) or Memapsin 2 and gamma (γ) secretase yields two β-amyloid peptide variants, Aβ 40 and Aβ 42. Aβ 42 is more prone to aggregation and hence makes up the bulk of the senile plaques [4,12,13,14]. According to the amyloid-cascade theory, agglutination of the β-amyloid forms the basis for the series of pathological events associated with Alzheimer's onset and progression [12,15,16]. These pathological events including cholinergic deficits, tau-hyperphosphorylation, microtubule disintegration, and neuronal damage culminate in cognitive impairment and ultimately AD [4].

Although β-amyloid fibrillization into insoluble senile plaques has been heralded for several decades to be critical in synaptic-collapse-mediated cognitive decline, emerging evidence shows that abnormal levels of the soluble non-fibrillar β-amyloid oligomer markedly diminishes long-term potentiation, an underlying molecular mechanism in learning and memory acquisition, and better correlates with Alzheimer's disease severity [16,17]. Furthermore, cholinergic deficits characterized by low levels of acetylcholine (Ach) in the synaptic cleft, elevated activities of acetylcholinesterase (AChE) and Butyrylcholinesterase (BuChE) have also been suggested to cause neuronal damage, a key player in AD pathophysiology.

Epidemiological studies have demonstrated that β-amyloid influences cholinesterase activities. However, increased activities of BuChE correspond more with AD advancement [9]. Therefore, therapeutic interventions targeted at attenuating the activities of β-secretase, improving cholinergic deficits through the inhibition of BuChE and AChE activities as well as disintegrating and clearing of the pathological lesions especially β-amyloid, have been suggested to ameliorate AD [4,14,18,19]. In recent times, treatment modalities for AD are broadly grouped into non-drug and drug interventions. The non-pharmacological interventions include music-based therapy, psychological treatment, and cognitive stimulation.

Whereas the pharmacological interventions consist of cholinesterase inhibitors; tacrine, galantamine, rivastigmine, donepezil, N-methyl-D-aspartate receptor antagonists (NMDA) memantine, antipsychotics; risperidone, and immunotherapies; aducanumab. These treatment modalities only modulate the symptoms and not the disease [20]. However, the disease-modifying drug, Aducanumab is restricted to specific AD patients, and it is also associated with very deleterious side effects known as amyloid-related imaging abnormalities (ARIA) [8,14]. These drawbacks, coupled with the idiosyncrasies of people living in rural areas to medicinal plants have turned the spotlight on medicinal plants.

The use of medicinal plants for healing is as old as mankind itself [21,22,23]. Medicinal plants with rich pharmacological compounds (phytochemicals) have become the subject of intense bioprospecting for novel therapeutics against numerous diseases including Alzheimer's disease [14,24]. South Africa displays an array of plant biodiversity and a few of these plants have been used in traditional medicine [14]. Traditional healers ubiquitously use herbal decoction made from the bark of *Ptaeroxylon obliquum* and *Bauhinia bowkeri* for AD treatment. *Bauhinia bowkeri* Harv, a Leguminosae, known as Kei White Bauhinia, Keibeesklou, and uMdlandlovu in English, Afrikaans, and Zulu, respectively, belongs to the large family Fabaceae and subfamily Caesalpiniodeae [24,25,26].

It is native to tropical regions across the globe but in South Africa, it is located at the thickets or Valley Bushveld in the Eastern Cape [27]. *B. bowkeri* can either be a tree or shrub but of average size. The leaves are conspicuously butterfly-like with two rounded nearly semi-circular lobes that are fused along the inner margin as if on a hinge [28]. Traditionally, *B. bowkeri* is used for skin beautification, steaming, bathing, inviting ancestral spirits as well as inducing vomiting [25]. In South Africa, the plant is used to treat gastrointestinal disturbances such as diarrhea and dysentery. The crude extracts of *B. bowkeri* have also been reported to exhibit anti-inflammatory, anti-microbial, and antioxidant activities [24].

Ptaeroxylon obliquum (Thunb.) Radlk, a Rutaceae and the only type of species in the genus Ptaeroxylon, is a dioecious plant that is indigenous to the eastern coastal part of South Africa and northwards to the Northern Province, including Zimbabwe, Mozambique, and Namibia [29,30]. *P. obliquum* commonly known as sneezewood and locally as Umthathi, has a whitish-grey bark that is smooth when young but becomes fissured as it ages. Its flowers have four petals surrounded by creamy white buds that are small

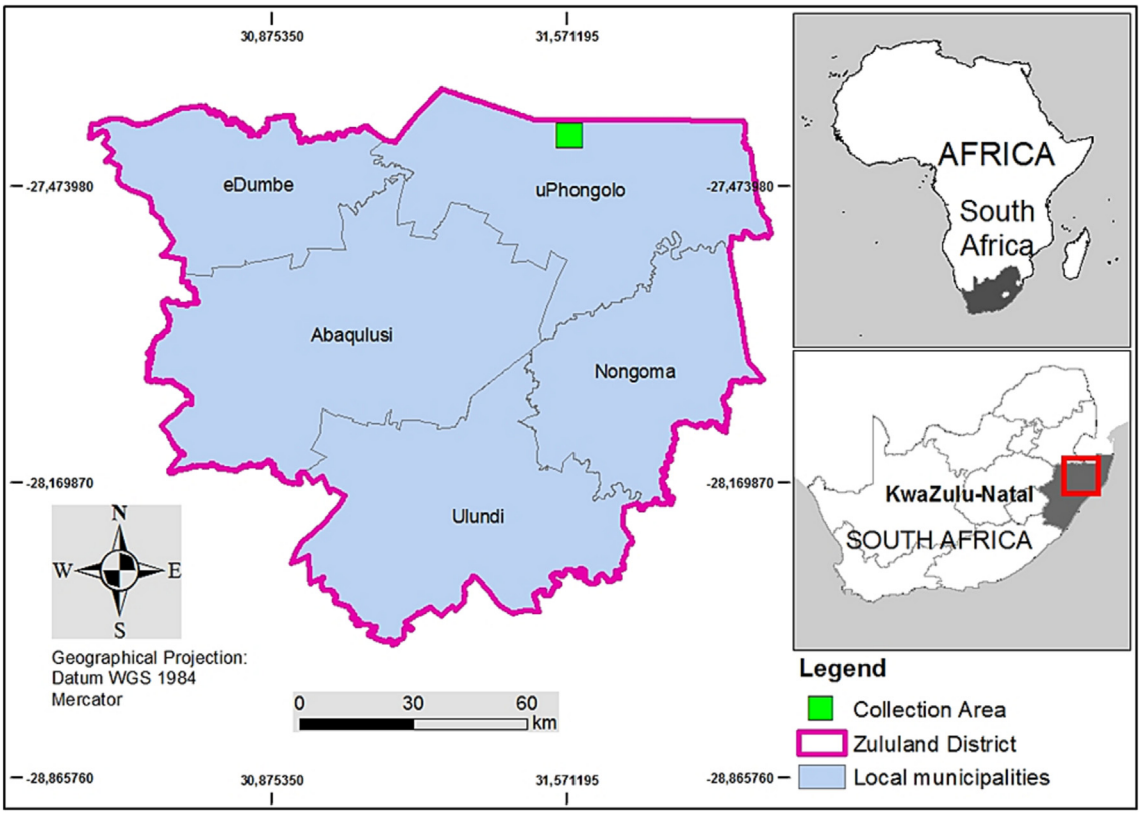

Fig. 1. Collection site of plant materials.

and sweetly scented [31]. The trees of this plant are of different sizes, but in montane forests, reach a height of 10 m.

The bark of *P. obliquum* is customarily used to treat animal and human diseases including lupus, rheumatism, ticks, and anthrax infection, whereas the pulverized bark is used as snuff for recreational purposes and analgesic for headaches, especially by people of Xhosa lineage. The acetone crude extracts of the leaves of *P. obliquum* have been demonstrated to possess anti-microbial, anti-hypertensive, and free radical scavenging properties [29,30]. Nevertheless, the anti-Alzheimer properties of these plants, *P. obliquum* and *B. bauhinia*, have not been scientifically validated, hence the study is aimed at evaluating the *in vitro* Alzheimer's disease-alleviating potentials of these plants.

In addition, *in silico* studies of the binding energy of the most abundant compounds identified by gas chromatography-mass spectroscopy (GC-MS) from both plants and standard compounds on some enzymes such as β-secretase 1 (Memapsin 2), AChE, and BuChE that have been implicated in AD pathophysiology were investigated.

2. Materials and methods

2.1. Chemicals

Analytical grade chemicals and commercial assay kits used in this study were purchased from Sigma Aldrich Co. LTD (Steinheim, Germany).

2.2. Plant collection

The plants were collected from uPhongolo (Fig. 1) KwaZulu Natal Province (27° 21′09.7″ S 31° 34′31.3″ E), South Africa. The names of the plants were accessed on January 16, 2021 from https://powo.science.kew.org. Both plants were identified, and authenticated, and their specimens are kept at the herbarium of the Department of Botany, University of Zululand. The plants were assigned specimen numbers V10 and V12 for *P. obliquum* and *B. bowkeri* respectively.

2.3. Plant extraction

The collected 549.13 g and 452.25 g dry weights of the stem barks of *B. bowkeri* and *P. obliquum*, respectively were cleaned, washed, and air-dried at room temperature. The pulverized samples were then sequentially extracted with hexane, dichloromethane (DCM), and 70% ethanol (1:5 W/V) on a Labcon orbital mechanical shaker (150 rpm; 25 °C) for 144 hr (48 hr for each solvent; each solvent was refreshed after 24 hr), to yield hexane, dichloromethane, and ethanol crude extracts, respectively. The different crude extracts were separately filtered through Whatman filter paper (no. 1) and concentrated *in vacuo*. Each crude extract was then kept in brown sterile bottles and stored in the refrigerator. For subsequent analysis, extracts were resuspended in ethanol.

2.4. Gas chromatography-mass spectrometer analysis

The phytochemical analysis of the crude extracts was performed with a Perkin-Elmer GC Clarus 500 system and gas chro-

Table 1
Enzymes and their protein data bank ID.

Protein/ Receptor	PDB ID
Acetylcholinesterase	1vot
Butyrylcholinesterase	7aiy
β-secretase	1xs7

matography connected to a mass spectrometer furnished with Elite-1, fused silica capillary column (30 mm × 0.25 mm 1DX 1 μMdf, composed of 100% Dimethyl poly Siloxane). Detection of compounds employs an electron ionization system with an ionization energy of 70 eV. The eluent (carrier) gas was helium, and this was used at a constant flow rate of 1 ml/min and an injection volume of 2 μl (split ratio of 10:1); injector temperature 250 °C; ion-source temperature 280 °C. The oven temperature was programmed to hold at 110 °C for 2 min, thereafter with an increase of 10 °C/min interval until it reaches 200 °C, then by 5 °C /min to 280 °C, ending with a 9 min isothermal at 280 °C. The mass spectra were obtained at 70 eV, a scan interval of 0.5 s, and fragments from 45 to 450 Da.

The overall running time of the GC was 36 min for each sample. The relative amount (%) of each component was calculated by comparing its average peak area to the total peak areas. Turbomass was the preferred choice of software for the mass spectra and chromatograms. The National Institute of Standards and Technology (NIST) with more than 62,000 patterns was adopted to interpret the GC-MS-derived mass spectrum. Determination of the name, molecular weight, and structure of each component in the plant materials was achieved by comparing the spectrum of the unknown component to that of the known components in the NIST library.

2.5. In silico studies

The prediction of the inhibition of compounds derived from the GC-MS analysis against proteins central to Alzheimer's disease pathogenesis was achieved using computational molecular docking studies. In this study, the proteins (Table 1) downloaded from the protein data bank (PDB) were simulated separately with each ligand-phytochemical (Table 2) using Autodock Vina on Pyrx virtual screening tool. Only the most abundant phytochemicals (area % ≥ 1.81) from the plants were considered for docking. Their 3D crystal structure was downloaded from PUBCHEM database in the .sdf format while that of the receptors/proteins was obtained as .pdb format. Only proteins with putative ligands without mutations were selected from the PDB.

The discovery studio visualizer (BIOVIA, 2020) was used for protein optimization (removal of water, non-standard amino acids, and chains for polymeric proteins) and generated the PDBQT for the receptor motif only before being docked. The lowest binding affinity energy (highest negative value) was taken from the docking results. The interaction of the complex (ligand and protein) was viewed using the BIOVIA Discovery Studio visualizer software. Only the figure of the ligands that inhibited the three proteins was depicted in the result section.

2.6. Fourier-transform infrared spectroscopy analysis

The functional groups of the crude extracts were ascertained by scanning using the FTIR spectrophotometer (Spectrum Two, PerkinElmer, USA) at a spectra range of 370–4000 cm^{-1} at room temperature. The functional groups were derived by comparing the peak frequencies to the IR spectroscopy correctional table.

2.7. Cholinesterase inhibitory activity assay

The modified method of Ellman [32] was adopted to assess the inhibitory activities of the crude extracts against BuChE and AChE. A reaction mixture containing 0.02 ml enzyme solution (1.2 KU), 0.1 ml phosphate buffer (0.1 M, pH 7 containing 6 mM $NaHCO_3$), 0.1 ml phosphate buffer (0.1 M, pH 7), 0.01 ml DNTB, and 0.02 ml of different crude extract concentrations (0–0.1 mg/ml) was incubated at 25 °C for 20 min. Thereafter, 0.01 ml butyrylcholine iodide was added and the change in absorbance was measured over time (5 min at 30 s intervals). Tacrine was used as the positive control. The enzyme activity was calculated as the change in absorbance/sec in the presence and absence of the crude extract before being expressed in percentage inhibition using [**Equation 1**]:

$$Inhibition(\%) = \frac{A_c - A_t}{A_c} \times 100 \quad (1)$$

where, A_c is the absorbance of the control and A_t is the absorbance in the presence of the extract. IC_{50} values of the extracts were determined using GraphPad Prism version 9.1.1.

A similar experimental set-up was used to investigate the AChE inhibitory activity of the crude extracts. Rat brain homogenate was used as the source of AChE and acetylthiocholine iodide (10 mM) was used in place of the butyrylthiocholine iodide.

Table 2
Secondary metabolites and their PubChem ID.

Compound/secondary metabolites	PUBCHEM ID
n-Hexadecanoic acid	985
9,12-Octadecadienoic acid, methyl ester	5284421
(*Z*)6, (*Z*)9-Pentadecadien-1-ol	5365570
Phytol	5280435
Cycloheptane, 4-methylene-1-methyl-2-(2-methyl-1-propen-1-yl)-1-vinyl-	572161
Spathulenol	13854255
Bicyclo [7.2.0] undec-4-ene, 4,11,11-trimethyl-8-methylene-, [1R(1R*,4Z,9S*)]-	5322111
8-(1,1-Dimethylallyl)-5,7-dimethoxycoumarin	621257
Cyclohexane, 1-ethenyl-1-methyl-2,4-bis(1-methylethenyl)-, [1S-(1. alpha.,2. beta.,4. beta.)]-	6431151
Bicyclo [5.2.0] nonane, 2-methylene-4,8,8-trimethyl-4-vinyl-	564746
9,12-Octadecadienoic acid (*Z, Z*)-	5280450
7-Tetradecenal, (*Z*)-	5364468
Heptanoic acid, 6,7-dimethoxy-2-oxo-2H-chromen-4-ylmethyl ester	536229
9,12,15-Octadecatrien-1-ol, (*Z, Z, Z*)-	6436081
9,12-Octadecadienoyl chloride, (*Z, Z*)-	9817754
Thunbergol	5363523
cis-Vaccenic acid	5282761
7-Hexadecenal, (*Z*)-	5364438
1,5,9-Cyclotetradecatriene, 1,5,9-trimethyl-12-(1-methylethenyl)-	328947
gamma. -Gurjunenepoxide-(2)	572103
Epiglobulol	11858788
Guaia-1(10),11-diene	520826
Tacrine	1935

Table 3
Percentage (%) yield of extracts.

Plant materials	Hexane	DCM	Ethanol
Ptaeroxylon obliquum	0.52	0.52	13.80
Bauhinia bowkeri	0.21	0.14	4.26

2.8. β-secretase inhibitory activity

The β-secretase inhibitory activity of the crude extracts was evaluated using a commercial assay kit (CS0010-1KT, Sigma) following the manufacturer's instructions.

2.9. β-amyloid ($A\beta_{1-42}$) peptide anti-aggregation property

The peptide (25 mM $A\beta_{1-42}$) was dissolved in 200 μl of 50 mM sodium hydroxide. After 3 min 700 μl of deionized pure water was added and the solution was made up to 1 ml with PBS (0.1 M pH 6.6) to make a final concentration of 25 μM. The solution

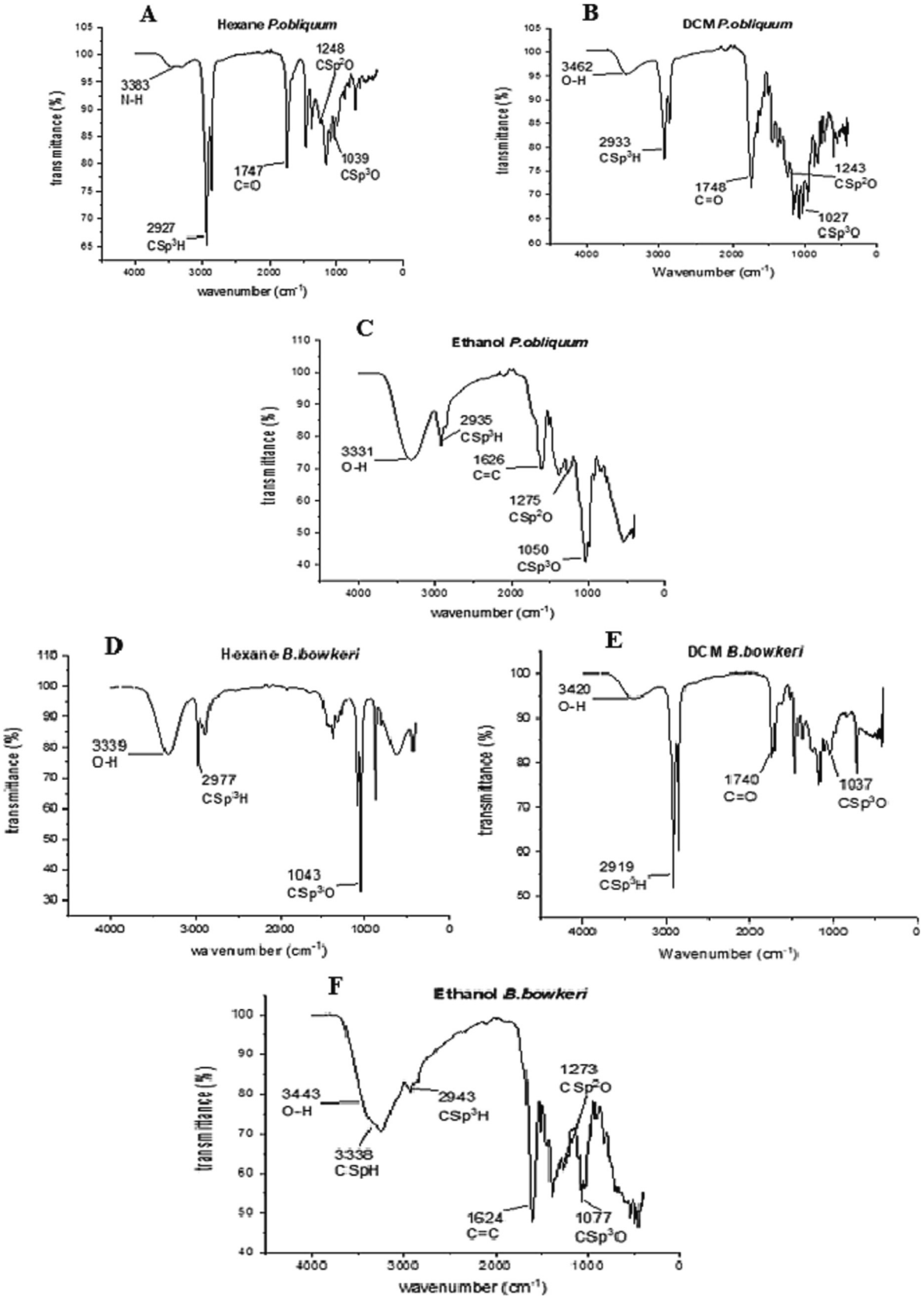

Fig. 2. Fourier transmission infrared spectroscopy of *Ptaeroxylon obliquum* and *Bauhinia bowkeri* extract. (A) Ethanol *P. obliquum* (B) DCM *P. obliquum* and (C) Hexane *P. obliquum* (D) Ethanol *B. bowkeri* (E) DCM *B. bowkeri* (F) Hexane *B. bowkeri.*

Table 4
Phytochemicals detected in *Bauhinia bowkeri* and *Ptaeroxylon obliquum* extracts.

Pharmacophore	Retention time (min)	Molecular formular	Molecular weight (g/mol)	*Bauhinia bowkeri* extracts			*Ptaeroxylon obliquum* extracts		
				Hexane	DCM	Ethanol	Hexane	DCM	Ethanol
n-Hexadecanoic acid	18.795	$C_{16}H_{32}O_2$	256.00	21.01	32.75	–	–	–	5.21
9,12-Octadecadienoic acid, methyl ester	23.656	$C_{19}H_{34}O_2$	294.47	–	24.1	–	–	–	–
(*Z*)6, (*Z*)9-Pentadecadien-1-ol	23.884	$C_{15}H_{28}O$	224.38	–	16.98	–	–	–	–
Phytol	22.489	$C_{20}H_{40}O$	296.00	–	4.37	–	–	–	–
9,12-Octadecadienoic acid (*Z, Z*)-	23.261	$C_{18}H_{32}O_2$	280.40	20.80	–	–	–	–	–
7-Tetradecenal, (*Z*)-	23.477	$C_{14}H_{26}O$	210.36	12.97	–	–	–	–	–
Heptanoic acid, 6,7-dimethoxy-2-oxo-2H-chromen-4-ylmethyl ester	22.619	$C_{19}H_{24}O_6$	348.40	7.59	–	–	–	–	–
9,12,15-Octadecatrien-1-ol, (*Z, Z, Z*)-	21.758	$C_{18}H_{32}O$	264.40	6.88	–	–	–	–	–
9,12-Octadecadienoyl chloride, (*Z, Z*)-	20.973	$C_{18}H_{31}ClO$	298.90	4.08	–	–	–	–	–
Cycloheptane, 4-methylene-1-methyl-2-(2-methyl-1-propen-1-yl)-1-vinyl-	23.214	$C_{15}H_{24}$	204.36	–	–	–	8.49	10.70	15.38
Spathulenol	21.635	$C_{15}H_{24}$	220.35	–	–	–	17.26	9.39	4.90
Epiglobulol	22.139	$C_{15}H_{26}O$	222.37	–	–	–	–	8.84	8.55
Bicyclo [7.2.0] undec-4-ene, 4,11,11-trimethyl-8-methylene-, [1R (1R*,4Z,9S*)]-	18.234	$C_{15}H_{24}$	204.35	–	–	–	–	5.80	–
8-(1,1-Dimethylallyl)-5,7-dimethoxycoumarin	30.085	$C_{16}H_{18}O_4$	274.31	–	–	–	–	3.40	4.29
Cyclohexane, 1-ethenyl-1-methyl-2,4-bis(1-methylethenyl)-, [1S-(1. alpha.,2. beta.,4. beta.)]-	18.354	$C_{15}H_{24}$	204.35	–	–	–	–	3.00	–
Bicyclo [5.2.0] nonane,2-methylene-4,8,8trimethyl-4-vinyl-	19.193	$C_{15}H_{24}$	204.35	–	–	–	–	2.47	–
9,12,15-Octadecatrienoic acid, 2,3-dihydroxypropyl ester, (*Z, Z, Z*)-	30.736	$C_{27}H_{44}O_2$	352.26	–	–	–	–	1.95	–
Thunbergol	22.189	$C_{20}H_{34}O$	290.50	–	–	–	5.73	–	–
cis-Vaccenic acid	23.501	$C_{18}H_{34}O_2$	282.50	–	–	–	4.73	–	–
1,5,9-Cyclotetradecatriene, 1,5,9-trimethyl-12-(1-methylethenyl)-	18.373	$C_{20}H_{32}$	272.50	–	–	–	2.64	–	–
gamma Gurjunenepoxide-(2)	17.527	$C_{15}H_{24}O$	220.35	–	–	–	2.04	–	–
Octadecanoic acid, 2-(2-hydroxyethoxy) ethyl ester	24.337	$C_{22}H_{44}O_4$	372.58	–	–	–	1.83	–	–
Guaia-1(10),11-diene	17.924	$C_{15}H_{24}$	204.35	–	–	–	1.81	–	–
Hexadecanoic acid, ethyl ester	18.85	$C_{18}H_{36}O_2$	284.48	–	–	–	–	–	7.70
7-Hexadecenal, (*Z*)-	23.979	$C_{16}H_{30}O$	238.41	–	–	–	–	–	3.03
Isopropyl linoleate	30.419	$C_{31}H_{38}O_2$	322.52	–	–	–	–	–	2.86

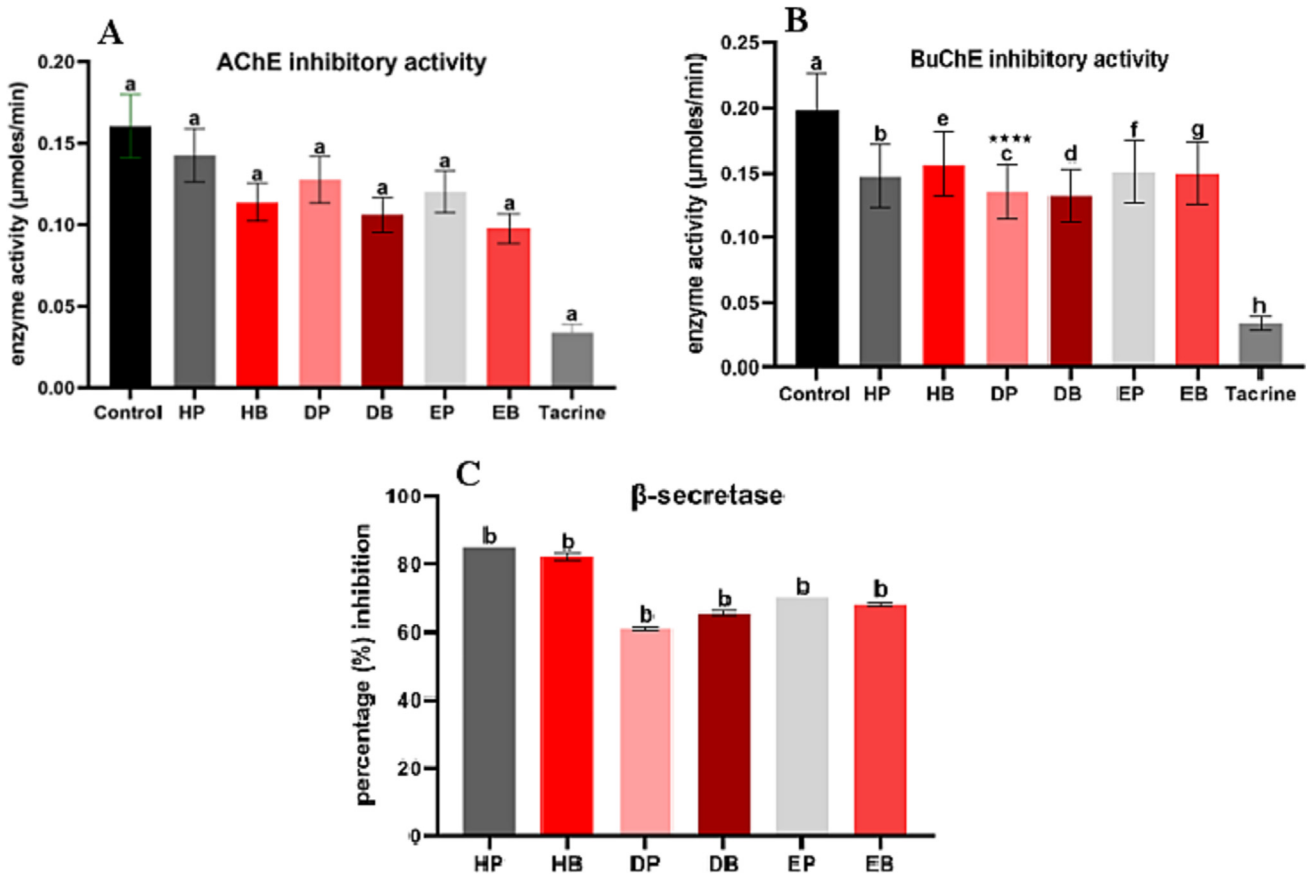

Fig. 3. Enzyme inhibition activity of the crude extracts. (A) AChE-Acetylcholinesterase (B) BuChE-Butyrylcholinesterase (C) β-secretase. Values are presented as mean ± standard deviation of mean (n = 3). Values with the asterisks $^{****}P < 0.005$.

Table 5
IC_{50} (μg/ml) of the hexane, DCM, and ethanol extracts of *P. obliquum* and *B. bowkeri*.

Crude extract	β-Secretase	AChE	BuChE
P. obliquum			
Hexane	29.5 ± 0.1[b]	77.01 ± 0.02[a]	4.79 ± 0.03[b]
DCM	41.1 ± 0.58[b]	66.59 ± 0.01[a]	1.77 ± 0.02[c****]
Ethanol	35.5 ± 0.1[b]	69.05 ± 0.01[a]	3.54 ± 0.04[d]
B. bowkeri			
Hexane	30.4 ± 1.15[b]	59.23 ± 0.01[a]	2.40 ± 0.03[e]
DCM	36.8 ± 0.58[b]	59.09 ± 0.01[a]	2.33 ± 0.01[f]
Ethanol	38.1 ± 0.58[b]	58.11 ± 0.01[a]	4.29 ± 0.01[g]
Tacrine	NA	46.20 ± 0.01[a]	6.02 ± 0.02[a]

Values are presented as mean ± standard deviation of mean (n = 3). Values with different superscript letters along the same column are significantly different ($P < 0.05$), **** $P < 0.00005$.

was then sonicated for 3 min and centrifuged at 4000 x g, for 20 min at 4 °C. Into the tubes containing 5 μM $A\beta_{1-42}$, the crude extracts (80 and 160 μg/ml) were added in the ratio 1:1. PBS was used in place of the extract in the negative control. The tubes were incubated at 37 °C and aliquots (10 μl) were taken at 0, 24, 48, 72, and 96 h for TEM and Th-T analysis.

2.10. Thioflavin-T (ThT) assay

This assay was used to evaluate Aβ aggregation and disaggregation properties of the crude extracts. A reaction mixture containing 10 μl of 1 mM Th-T solution (prepared in 50 mM glycine-NaOH buffer of pH 8.5) and 5 μl of the interval collected aliquots was vortexed for 10 s. Thioflavin fluorescence intensity signals were measured using a microtiter plate reader (Glomax-Discover Promega) at 450 nm (excitation) and 480 nm (emission). The negative control was without the extract, whereas, Th-T and PBS (0.1 M, pH 6.6) were used as blank [18,33].

2.11. Transmission electron microscopy (TEM)

TEM imaging was used to determine the presence and absence of Aβ aggregates. A 2% uranyl acetate was used to negatively stain the carbon-coated copper grid after aliquots (10 μl) of the incubated $A\beta_{1-42}$ solution were placed on it. The stained grid was left to dry for 1 hr before being scanned under TEM. The effect of the most active extract (160 μg/ml) of *B. bowkeri* on Aβ aggregation was further investigated following a similar experimental procedure. The $A\beta_{1-42}$ was incubated alone for 48 hr after which the extract was added. The sampling and testing of aliquots continued until 96 hr. The negative control was without the extract throughout the experiment.

2.12. Statistical analysis

All the experiments conducted were triplicated and the results were expressed as mean ± standard error of the mean. Graph pad prism 9.01 was used to determine the analysis of variance (ANOVA), where values of $P \leq 0.05$ were assumed to be statistically significant.

3. Results

3.1. Percentage (%) yield

The result (Table 3) shows that both plants contained components that were more extractable in the ethanol than the other solvents used. *P. obliquum* has a higher yield between both plants.

3.2. FTIR

The result of the FTIR analysis highlights predominantly the presence of O—H, C═O, CSp^3H, CSp^3O, and CSp^2O functional groups despite the different patterns/peaks observed within and between the crude extracts of both plants (Fig. 2A–F). Interestingly, only the

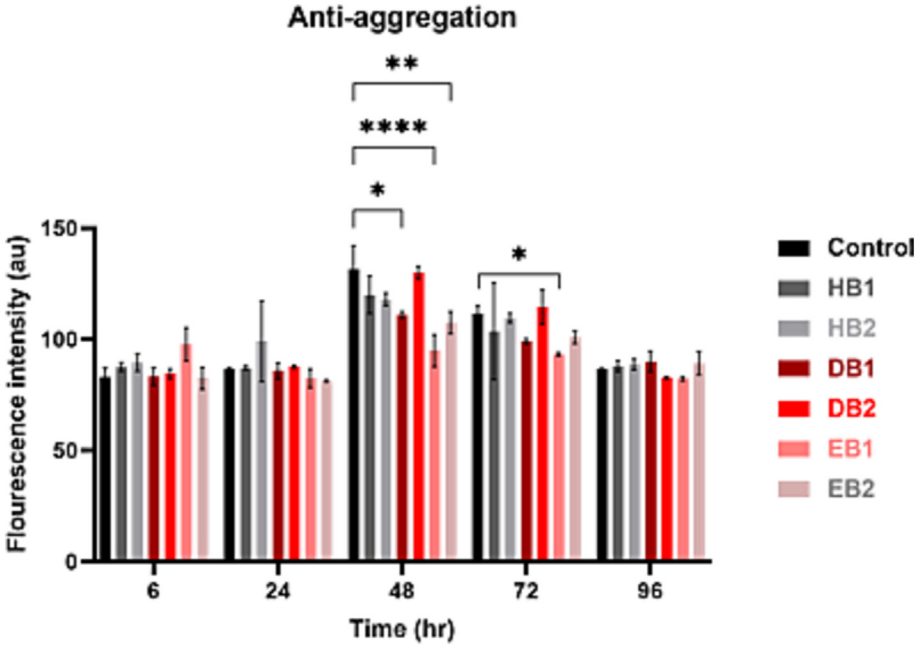

Fig. 4. Aβ aggregation inhibition of the crude extracts of the plants using Thioflavin-T assay measured over time (fluorescent intensity (Au)/ time) (hr). Control: Aβ alone; HB: *Bauhinia bowkeri* hexane extract; EB: *Bauhinia bowkeri* ethanol extract; DB: *Bauhinia bowkeri* dichloromethane extract. 1 and 2 refers to Conc 1–160 μg/ml, Conc 2–80 μg/ml. Values are presented as mean ± standard deviation of mean (n = 3). Values with the asterisks *$P < 0.05$, **$P < 0.005$, ****$P < 0.00005$ shows significant difference compared to the control.

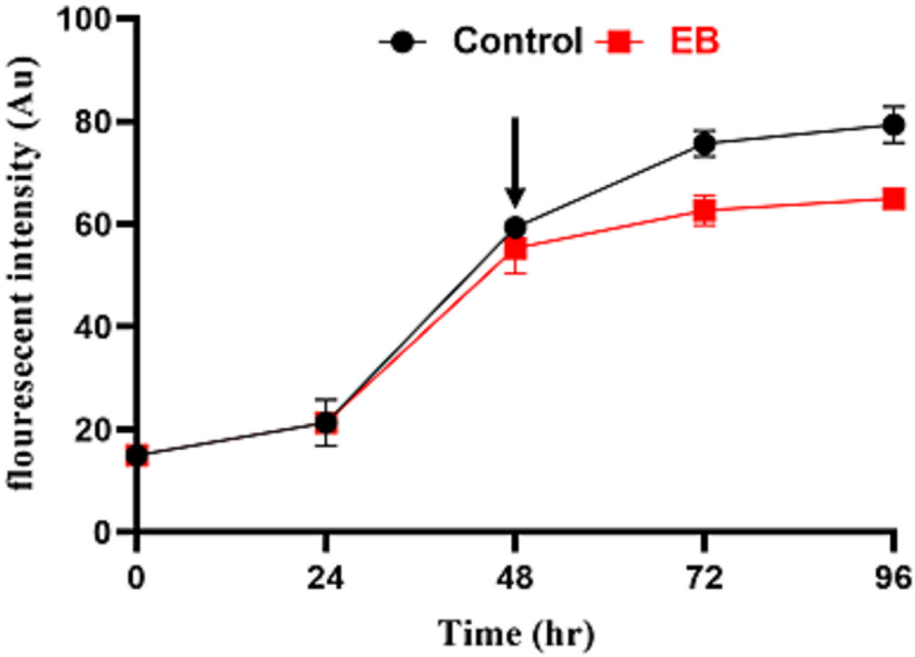

Fig. 5. Anti-aggregation effect of *B. bowkeri* ethanol extract on $A\beta_{1-42}$ using the Th-T fluorescence assay. Incubation of the $A\beta_{1-42}$ alone enhanced the formation of Aβ oligomers and fibrils as revealed by the increase in fluorescent intensity. However, the deviation or drift of the extract graph from the control graph after the addition of the extract, is a pointer that the ethanol extract destabilized the preformed Aβ aggregates. Control: $A\beta_{1-42}$ alone; EB: *B. bowkeri* ethanol extract (160 μg/ml). The arrow is an indication of the time (48 h) the extract was added to the reaction mixture.

hexane extract of *P. obliquum* contains the N—H functional group belonging to the secondary amine (Fig. 2C).

3.3. GC-MS analysis of the crude extracts

The GC-MS screening of the phytochemical composition of the crude extracts (hexane, DCM, and 70% ethanol) of *P. obliquum* and *B. bowkeri* revealed the presence of diverse phytochemicals within and between both plants, nonetheless. Over 230 phytochemicals were identified however, only the most abundant compounds (not < 1.81) in both plants are listed in Table 4. The result shows that n-Hexadecanoic acid was the most abundant phytochemical in *B. bowkeri* (DCM extract, 32.75%), although it is also found in the ethanol extract of *P. obliquum*, but at low concentration (ethanol extract, 5.21%).

On the other hand, spathulenol had the highest % abundance in *P. obliquum* (hexane extract, 17.26%) and it is specific to only *P. obliquum*. Certain compounds were also peculiar to specific extracts of each plant for instance, 1,5,9-Cyclotetradecatriene, 1,5,9-trimethyl-12-(1-methylethenyl)-, Bicyclo [5.2.0] nonane, 2-methylene-4,8,8-trimethyl-4-vinyl-, Isopropyl linoleate were only found in the hexane, DCM, and ethanol extract of *P. obliquum*,

Table 6
Binding affinity of phytochemicals to 1vot, 1xs7 and 7aiy proteins.

Pharmacophore	Binding affinity (Kcal/mol^{-1}) 1vot	1xs7	7aiy
Bicyclo [5.2.0] nonane, 2-methylene-4,8,8-trimethyl-4-vinyl-	−8.8	−7.2	−7.4
Bicyclo [7.2.0] undec-4-ene, 4,11,11-trimethyl-8-methylene-, [1R-(1R*,4Z,9S*)]-	8.6	−7.3	−7.7
Cycloheptane, 4-methylene-1-methyl-2-(2-methyl-1-propen-1-yl)-1-vinyl-	−7.7	−7.5	−6.9
Cyclohexane, 1-ethenyl-1-methyl-2,4-bis(1-methylethenyl)-, [1S-(1. alpha.,2. beta.,4. beta.)]-	−7.9	−6.8	−6.7
1,5,9-Cyclotetradecatriene, 1,5,9-trimethyl-12-(1-methylethenyl)-	−9.2	−8.8	−8.7
8-(1,1-Dimethylallyl)-5,7-dimethoxycoumarin	−8.5	−7.2	−7.7
Epiglobulol	−9	−7.3	−7.7
.gamma.-Gurjunenepoxide-(2)	−8.6	−7.6	−7.5
Guaia-1(10),11-diene	−8.8	−7.6	−7.8
Heptanoic acid, 6,7-dimethoxy-2-oxo-2H-chromen-4-ylmethyl ester	−9	−6.9	−7.9
n-Hexadecanoic acid	−6.5	−5.8	−5.9
7-Hexadecenal, (*Z*)-	−5.9	−5.2	−5.8
9,12-Octadecadienoic acid (*Z, Z*)-	−7.1	−5.8	−6.5
9,12-Octadecadienoyl chloride, (*Z, Z*)-	−7.1	−6.2	−6.4
9,12-Octadecadienoic acid, methyl ester	−6.6	−6	−5.9
9,12,15-Octadecatrien-1-ol, (*Z, Z, Z*)-	−7.2	−5.7	−5.8
(*Z*)6, (*Z*)9-Pentadecadien-1-ol	−6.6	−5.5	−5.7
Phytol	−8.1	−6.5	−6.3
Spathulenol	−8.5	−7.8	−7.8
Tacrine	−8.3	−7.7	−8
7-Tetradecenal, (*Z*)-	−6.4	−5.2	−5.5
Thunbergol	−8.4	−8.4	−8.3
cis-Vaccenic acid	−7.1	−5.8	−6.0

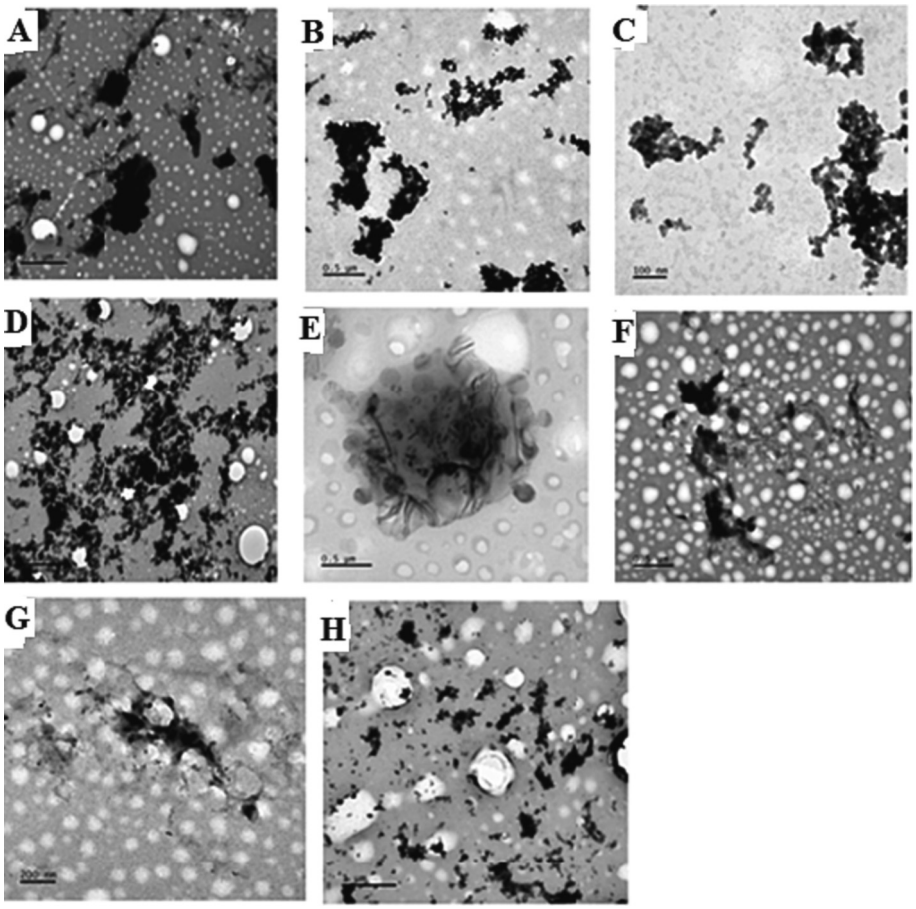

Fig. 6. Transmission electron microscope (TEM) images describing the effect of the ethanol crude extract (160 µg/ml) on the generation of $A\beta_{1-42}$ aggregates. The TEM images show the formation of fibrils from 24 h and became very conspicuous at 96 h of incubating the $A\beta_{1-42}$ alone. Contrastingly, the ethanol extract countered the oligomerization and fibrillization of the $A\beta_{1-42}$. (A) $A\beta_{1-42}$ alone at 24 h; (B) $A\beta_{1-42}$ alone at 48 h; (C) $A\beta_{1-42}$ alone at 72 hr (D) $A\beta_{1-42}$ alone at 96 h; (E) $A\beta_{1-42}$ incubated with *B. bowkeri* ethanol extract at 24 h; (F) $A\beta_{1-42}$ incubated with *B. bowkeri* ethanol extract at 48 h; (G) $A\beta_{1-42}$ incubated with *B. bowkeri* ethanol extract at 72 h; (H) $A\beta_{1-42}$ incubated with *B. bowkeri* ethanol extract at 96 h.

respectively. Similarly, the hexane and DCM extract of *B. bowkeri* contained 9,12-Octadecadienoic acid (Z, Z)-, and Phytol, respectively (Table 4).

3.4. β-secretase activity inhibition

The results demonstrated that the crude extracts possessed β-secretase inhibitory potential though the hexane crude extract of *P. obliquum* had the lowest IC_{50} value, there was no significant difference in their β-secretase inhibition activity (Fig. 3, Table 5).

3.5. Cholinesterase activity inhibition

All the crude extracts of the plants attenuated the activities of both AChE and BuChE (Fig. 3, Table 5), however they were more potent inhibitors of butyrylcholinesterase activity. While the ethanol crude extract of *B. bowkeri* was the most efficacious against AChE activities, the DCM crude extracts of both plants exhibited the highest anti-Butyrylcholinesterase activities, nonetheless, *P. obliquum* was a better inhibitor.

3.6. Anti-aggregation property of crude extract

The Th-T result presented in Fig. 3 showed that only the crude extracts of *B. bowkeri* possessed $A\beta_{1-42}$ aggregation attenuation property and the higher concentration (160 µg/ml) of the ethanol extract displayed the most efficacious effect when compared to the hexane and DCM extract of the same plant. The result also highlighted that the ethanol extract (160 µg/ml) exhibited the best $A\beta_{1-42}$ disaggregation activities with very great and slight significant differences at 48 and 72 hr, respectively when compared to the control (Fig. 4). Similarly, the TEM images were consistent with the trend observed with the result from Th-T assay (Fig. 5). The result of *P. obliquum* was not included because the extracts showed no significant $A\beta_{1-42}$ aggregation activity.

3.7. Computational (in silico) studies

The result of the molecular docking that is, the ligand-receptor interaction revealed that the phytochemical 1,5,9-Cyclotetradecatriene, 1,5,9-trimethyl-12-(1-methylethenyl)- (hereafter cyclotetradecatriene) had the lowest binding energy which is tantamount to the greatest binding affinity (Table 6) with all the selected proteins (1vot, 1xs7 and 7aiy) hence was the most potent inhibitor. Another compound, thunbergol displayed a strong binding affinity across all receptors/proteins. Worthy of note also is the fact that some compounds such as spathulenol, epiglobulol, Guaia-1(10),11-diene, gamma gurjunenepoxide-(2), 8-(1,1-dimethylallyl)-5,7-dimethoxy coumarin, and Bicyclo [5.2.0] nonane, 2-methylene-4,8,8-trimethyl-4-vinyl exhibited high binding affinity, but they are protein/receptor specific (Table 6). Furthermore, the separate interactions of tacrine, thun-

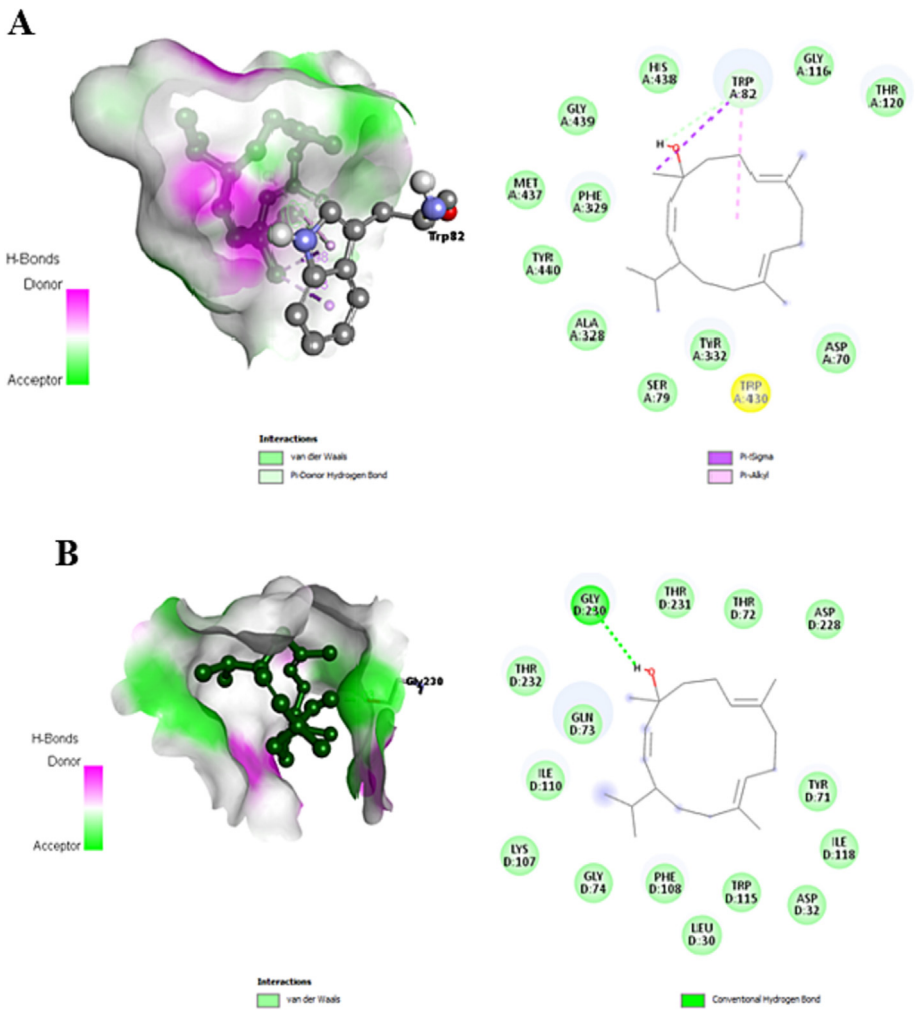

Fig. 7. Discovery Studio Visualizer analysis of the 3D and 2D complex formed by the compound (tacrine, thunbergol and Cyclotetradecatriene) and protein/receptor (AChE-1vot, BuChE-7aiy, and 1xs7-BACE1) separately. (A) Thunbergol-7aiy complex (B) Thunbergol-1xs7 complex (C) Thunbergol – 1vot complex (D) Tacrine-7aiy complex (E) Tacrine-1xs7 complex (F) Tacrine-1vot complex (G) Cyclotetradecatriene – 7aiy complex (H) Cyclotetradecatriene – 1xs7 complex (I) Cyclotetradecatriene – 1vot complex.

bergol and cyclotetradecatriene with the amino acids in the protein cavity led to the different types and number of bonds formed (Fig. 7A–I) and consequently the binding affinity displayed (Table 6).

4. Discussion of findings

Alzheimer's disease is a progressive neurodegenerative disorder that is multifactorial [8,34]. However, accumulated evidence has demonstrated that aggregation of Aβ peptide into senile plaques is the chief cornerstone in AD pathophysiology [6,16,17,35]. Abnormal production of Aβ mediates its accumulation and consequent aggregation culminating in AD pathogenesis. BACE-1 (β-secretase-1) is the enzyme that controls the rate-limiting step in the amyloidogenic pathway hence, keeping elevated activities of Memapsin 2 under control could also play a crucial role in AD onset and progression [4,14]. It is apparent therefore that attenuation of β-secretase activities and inhibiting the diverse forms of Aβ aggregates have emerged as an interesting therapeutic target for slowing down and/or even possibly eradicating AD [4,12].

In silico studies, enable the prediction of the inhibition of specific enzymes linked to a disease by a compound or molecule. It is therefore inevitable in novel drug design, repositioning, or repurposing of drugs [36,37,38,39]. Molecular docking (*in silico* studies) entails software to predict the best conformation or pose of a ligand or molecule in the binding cavity, pocket, or site of protein/receptor [40,41]. The best conformation or pose corresponds with the lowest binding energy (Kcal/mol), while the ligand-protein/receptor complex formed is analyzed using different software packages [41].

In this study, the compound was simulated with AChE, BuCHE, and β-secretase 1. Few of the phytochemicals (cyclotetradecatriene, thunbergol, Bicyclo [5.2.0] nonane, epiglobulol, Guaia-1 (10),11-diene) possessed inhibitory activities against these proteins, whereas cyclotetradecatriene and thunbergol attenuated all the proteins, other compounds exhibited protein-specific inhibition (Table 6). To this end, only the 2D and 3D structures of the complexes generated separately by tacrine, thunbergol, and cyclotetradecatriene with each of the proteins were represented using the discovery studio visualizer (Fig. 7A–I). This suggests that the compounds could possess anti-AD pharmacological activities and hence become a target of novel drug discovery [37,40,41].

The extract of *B. bowkeri* was not only able to inhibit aggregation of the Aβ fibrils but also mitigated its clumping (Fig. 4, Fig. 5, Fig. 6). However, both plants exhibited inhibitory effects on Memapsin 2 activity (Table 5) thus suggesting that while both

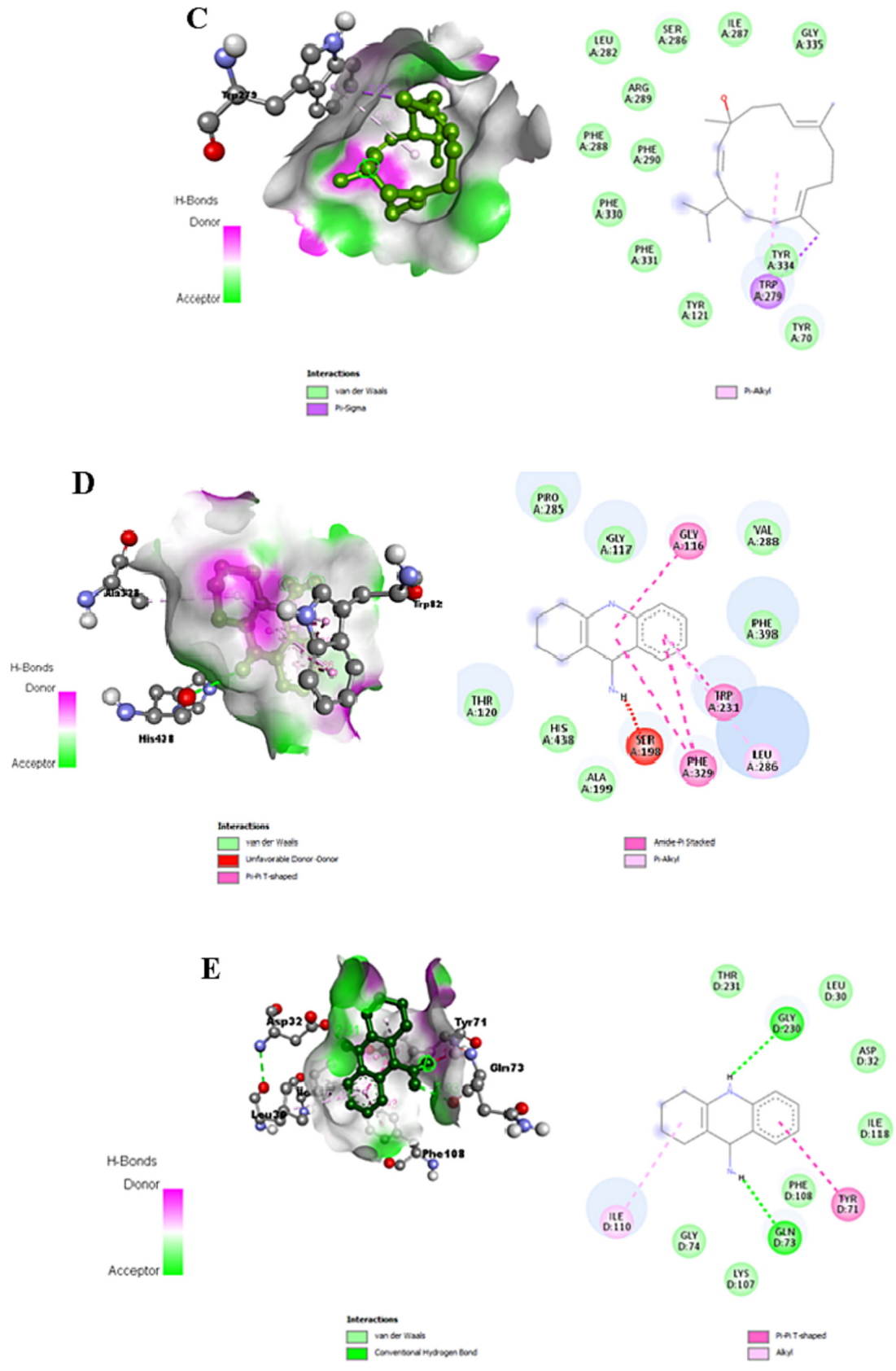

Fig. 7 (*continued*)

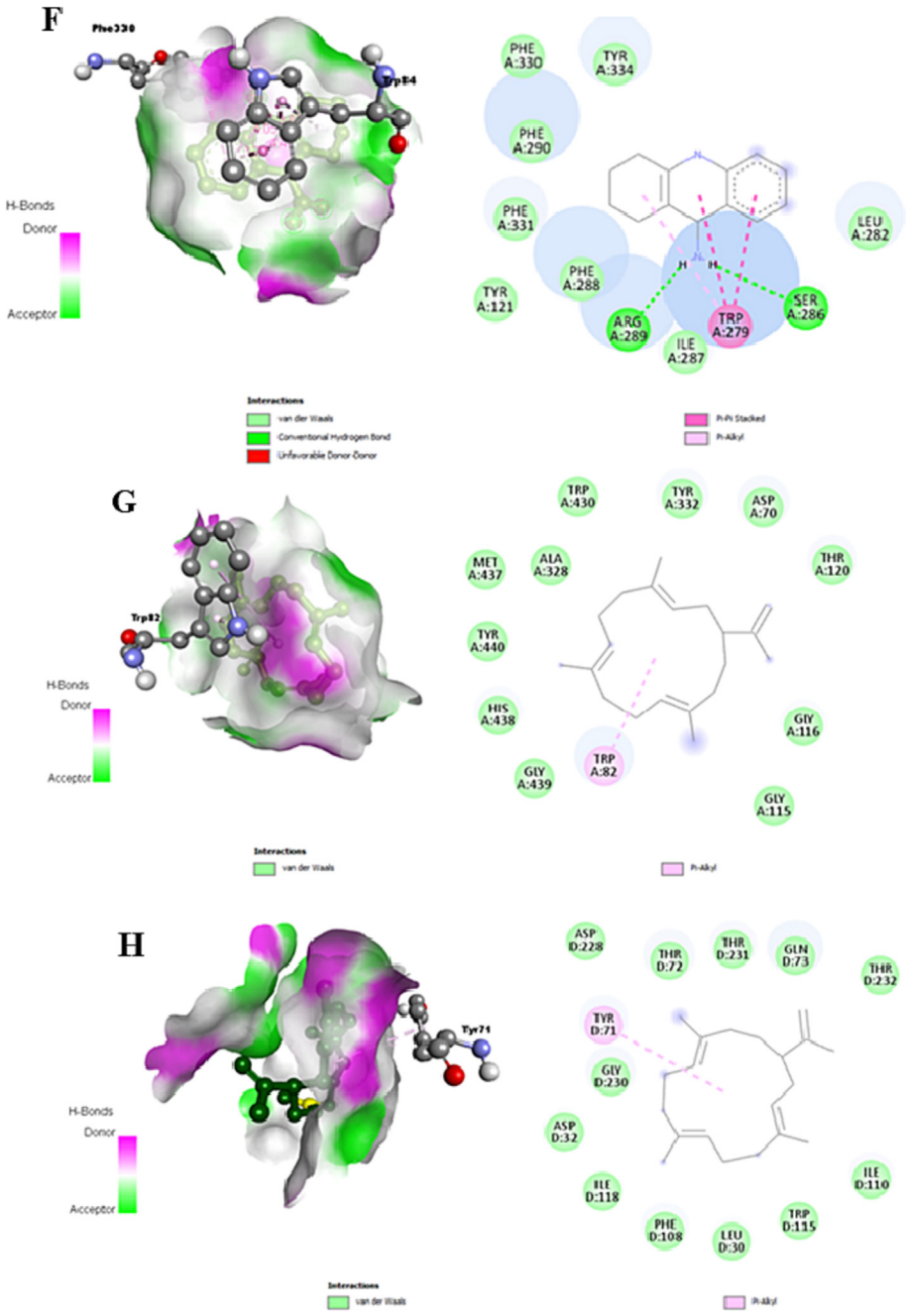

Fig. 7 (*continued*)

plants could delay AD development, only *B. bowkeri* could arrest Aβ aggregation-induced AD pathology. Similar findings (inhibition of β-secretase activities and disaggregation of fibrils) have been reported of some extracts of other plants; *Capsicum annuum* [18], Chlorella *sorokiniana* and *Chlorella minutissima* [33], black sesame [42], *Centella asiatica*, *Xysmalobium undulatum*, *Cussonia paniculate*, *Catha edulis* [14].

Cholinergic deficits caused by hyperactivities of AChE and BuChE leads to dysfunctional synaptic plasticity and impairs long-term potentiation ultimately contributing to cognitive decline, the main clinical manifestation of Alzheimer's disease [43,44]. The plants exhibited AChE and BuChE activities lowering potential (Fig. 3, Table 5). Interestingly, both plants had greater BuChE inhibitory activities (Table 5). Since the activities of BuChE correlate more with AD severity than AChE activity, and its inhibition has little or no effect on the neuromuscular junction and parasympathetic autonomous nervous system, its inhibition is therefore of more significant than AChE [44]. Literature reports that improved cholinergic transmission through decreasing AChE and BuChE activities restores cognition and consequently alleviates AD [4,43].

The therapeutic potential of *Ptaeroxylon obliquum* and *Bauhinia bowkeri* extracts relevant for the management of AD that has been revealed in this study is attributed to the phytochemical constituents of the plants (Fig. 2 and Table 4). Although the mechanism of the inhibition of aggregation is not understood, it is apparent that the extracts contained some compounds (8-(1,1-Di methylallyl)-5,7-dimethoxycoumarin, Spathulenol, Epiglobulol, Guaia-1(10),11-diene, n-Hexadecanoic acid, Thunbergol, Cyclotetradecatriene, Bicyclo[7.2.0]undec-4-ene, 4,11,11-trimethyl-8-met

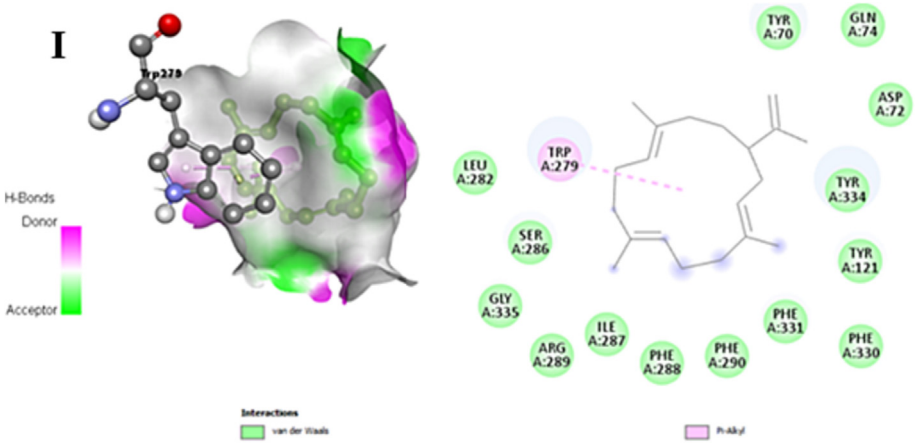

Fig. 7 (*continued*)

hylene-,[1R-(1R*,4Z,9S*)], gamma gurjunenepoxide-2) that have been reported to exhibit modulation of abnormal conditions such as oxidative stress, protein aggregation, and chronic inflammation associated with Alzheimer's onset and progression [45,46,47,48,49].

5. Conclusions

The study confirms the anti-cholinesterase and β-secretase inhibitory properties of these plants, while only *B. bowkeri* exhibited anti-aggregation potential, thus making them an excellent new drug bioprospecting for AD treatment. In addition, the molecular docking outcome prompted potential study into the isolation and characterization of the bioactive compound in the ethanol extract of *B. bowkeri*.

Ethical approval

The research project was approved by the ethics committee of the University of Zululand and assigned the certificate number: UZREC171110-030 Dept 2020/17.

Authors contributions

- Study conception and design: AR Opoku; RA Mosa; N Revaprasadu.
- Data collection: MC Ojo.
- Analysis and interpretation of results: MC Ojo.
- Draft manuscript preparation: MC Ojo; FO Osunsanmi; RA Mosa.
- Revision of the results and approval of the final version of the manuscript: AR Opoku; RA Mosa; N Revaprasadu; FO Osunsanmi; MC Ojo.

Financial support

The research did not receive any specific grants from funding agencies in the public, commercial, or not-for-profit sectors.

Conflict of interest

Michael Chukwuka Ojo reports financial support, article publishing charges, and travel were provided by University of Zululand Faculty of Science Agriculture and Engineering. Michael Chukwuka Ojo reports a relationship with University of Zululand Faculty of Science Agriculture and Engineering that includes: travel reimbursement. None has patent None pending to None. There are no additional activities to declare

Acknowledgments

We acknowledge the staff of the microscopy and microanalysis unit of the University of KwaZulu Natal Pietermaritzburg for the TEM image analysis, colleagues in the laboratory for their constructive criticism and invaluable input to the work.

Supplementary material

https://doi.org/10.1016/j.ejbt.2023.11.004.

Data availability

Data will be made available on request.

References

[1] Zhu Z, Lin Y, Li X, et al. Shared genetic architecture between metabolic traits and Alzheimer's disease: A large-scale genome-wide cross-trait analysis. Hum Genet 2019;138:271–85. https://doi.org/10.1007/s00439-019-01988-9. PMid: 30805717.
[2] Bonfili L, Cecarini V, Berardi S, et al. Microbiota modulation counteracts Alzheimer's disease progression influencing neuronal proteolysis and gut hormones plasma levels. Sci Rep 2017;7(1):2426. https://doi.org/10.1038/s41598-017-02587-2. PMid: 28546539.
[3] Guerreiro R, Hardy J. Genetics of Alzheimer's disease. Neurotherapeutics 2014;11:732–7. https://doi.org/10.1007/s13311-014-0295-9. PMid: 25113539.
[4] Agis-Torres A, Sollhuber M, Fernandez M, et al. Multi-target-directed ligands and other therapeutic strategies in the search of a real solution for Alzheimer's disease. Curr Neuropharmacol 2014;12(1):2–36. https://doi.org/10.2174/1570159X113116660047. PMid: 24533013.
[5] Zhao Y, Gong CX. From chronic cerebral hypoperfusion to Alzheimer-like brain pathology and neurodegeneration. Cell Mol Neurobiol 2015;35:101–10. https://doi.org/10.1007/s10571-014-0127-9. PMid: 25352419.
[6] Ayton S, Lei P, Bush AI. Metallostasis in Alzheimer's disease. Free Radic Biol Med 2013;62:76–89. https://doi.org/10.1016/j.freeradbiomed.2012.10.558. PMid: 23142767.
[7] Tampi RR. Paired associative stimulation (PAS) and Alzheimer's disease (AD). Int Psychogeriatr 2023;35(3):123–5. https://doi.org/10.1017/S1041610222000813. PMid: 36098440.
[8] 2023 Alzheimer's disease facts and figures. Alzheimers & Dementia 2023;19 (4):1598–1695. https://doi.org/10.1002/alz.13016 PMid: 36918389.
[9] Viayna E, Coquelle N, Cieslikiewicz-Bouet M, et al. Discovery of a potent dual inhibitor of acetylcholinesterase and butyrylcholinesterase with antioxidant activity that alleviates Alzheimer-like pathology in old APP/PS1 mice. J Med Chem 2020;64(1):812–39. https://doi.org/10.1021/acs.jmedchem.0c01775. PMid: 33356266.

[10] Ajala A, Uzairu A, Shallangwa GA, et al. Structure-based drug design of novel piperazine containing hydrazone derivatives as potent Alzheimer inhibitors: Molecular docking and drug kinetics evaluation. Brain Disorders 2022;7:100041. https://doi.org/10.1016/j.dscb.2022.100041.
[11] Abraha A, Ghoshal N, Gamblin TC, et al. C-terminal inhibition of tau assembly in vitro and in Alzheimer's disease. J Cell Sci 2000;113(21):3737–45. https://doi.org/10.1242/jcs.113.21.3737. PMid: 11034902.
[12] Hong L, Turner III RT, Koelsch G, et al. Memapsin 2 (β-secretase) as a therapeutic target. Biochem Soc Trans 2002;30(4):530–4. https://doi.org/10.1042/bst0300530. PMid: 12196130.
[13] Amani M, Shokouhi G, Salari AA. Minocycline prevents the development of depression-like behavior and hippocampal inflammation in a rat model of Alzheimer's disease. Psychopharmacology (Berl) 2019;236(4):1281–92. https://doi.org/10.1007/s00213-018-5137-8. PMid: 30515523.
[14] Thakur A, Chun YS, October N, et al. Potential of South African medicinal plants targeting the reduction of Aβ42 protein as a treatment of Alzheimer's disease. J Ethnopharmacol 2019;231:363–73. https://doi.org/10.1016/j.jep.2018.11.034. PMid: 30496841.
[15] Hook V, Schechter I, Demuth HU, et al. Alternative pathways for production of β-amyloid peptides of Alzheimer's disease. Biol Chem 2008;389(8):993–1006. https://doi.org/10.1515/BC.2008.124. PMid: 18979625.
[16] Hardy J, Selkoe DJ. The amyloid hypothesis of Alzheimer's disease: Progress and problems on the road to therapeutics. Science 2002;297(5580):353–6. https://doi.org/10.1126/science.1072994. PMid: 12130773.
[17] Westmark CJ. What's hAPPening at synapses? The role of amyloid β-protein precursor and β-amyloid in neurological disorders. Mol Psychiatry 2013;18(4):425–34. https://doi.org/10.1038/mp.2012.122. PMid: 22925831.
[18] Ogunruku OO, Oboh G, Passamonti S, et al. *Capsicum annuum* var. grossum (Bell pepper) inhibits β-secretase activity and β-amyloid1–40 aggregation. J Med Food 2017;20(2):124–30. https://doi.org/10.1089/jmf.2016.0077. PMid: 28098506.
[19] Sobhani R, Pal AK, Bhattacharjee A, et al. Screening indigenous medicinal plants of northeast India for their anti-Alzheimer's properties. Pharmacognosy Journal 2017;9(1):46–54. https://doi.org/10.5530/pj.2017.1.9.
[20] Coimbra JR, Marques DF, Baptista SJ, et al. Highlights in BACE1 inhibitors for Alzheimer's disease treatment. Front Chem 2018;6:178. https://doi.org/10.3389/fchem.2018.00178. PMid: 29881722.
[21] Adeola HA, Sabiu S, Aruleba RT, et al. Phytodentistry in Africa: Prospects for head and neck cancers. Clin Phytosci 2021;7(1):17. https://doi.org/10.1186/s40816-021-00254-8.
[22] Stojanoski N. Development of health culture in Veles and its region from the past to the end of the 20th century. Veles: Society of science and art 1999:13-34.
[23] Kelly K. In: The History of Medicine: Early Civilizations, Prehistoric Times to 500 CE. Ferguson Publishing Company; 2009. p. 174.
[24] Ahmed AS, Elgorashi EE, Moodley N, et al. The antimicrobial, antioxidative, anti-inflammatory activity and cytotoxicity of different fractions of four South African *Bauhinia* species used traditionally to treat diarrhoea. J Ethnopharmacol 2012;143(3):826–39. https://doi.org/10.1016/j.jep.2012.08.004. PMid: 22917809.
[25] Ndawonde BG, Zobolo AM, Dlamini ET, et al. A survey of plants sold by traders at Zululand muthi markets, with a view to selecting popular plant species for propagation in communal gardens. Afr J Range Forage Sci 2007;24(2):103–7. https://doi.org/10.2989/AJRFS.2007.24.2.7.161.
[26] Baloyi IT, Cosa S, Combrinck S, et al. Anti-quorum sensing and antimicrobial activities of South African medicinal plants against uropathogens. S Afr J Bot 2019;122:484–91. https://doi.org/10.1016/j.sajb.2019.01.010.
[27] Van Jaarsveld E. Veld gardening in South Africa. Veld Flora 1996;82(2):52–6.
[28] Khare P, Kishore K, Sharma DK. Historical aspects, medicinal uses, phytochemistry and pharmacological review of *Bauhinia variegate*. Asian J Pharm Pharmacol 2018;4(5):546–62. https://doi.org/10.31024/ajpp.2018.4.5.3.
[29] Ramadwa TE, McGaw LJ, Adamu M, et al. Anthelmintic, antimycobacterial, antifungal, larvicidal and cytotoxic activities of acetone leaf extracts, fractions and isolated compounds from *Ptaeroxylon obliquum* (Rutaceae). J Ethnopharmacol 2021;280:114365. https://doi.org/10.1016/j.jep.2021.114365. PMid: 34175445.
[30] Van Wyk C, Botha FS, Vleggaar R, et al. Obliquumol, a novel antifungal and a potential scaffold lead compound, isolated from the leaves of *Ptaeroxylon obliquum* (sneezewood) for treatment of Candida albicans infections. Suid-Afrikaanse Tydskrif vir Natuurwetenskap en Tegnologie 2018;37(1):1–5.
[31] Mwinga JL, Makhaga NS, Aremu AO, et al. Botanicals used for cosmetic purposes by Xhosa women in the Eastern Cape, South Africa. S Afr J Bot 2019;126:4–10. https://doi.org/10.1016/j.sajb.2019.03.038.
[32] Gorun V, Proinov I, Băltescu V, et al. Modified Ellman procedure for assay of cholinesterases in crude enzymatic preparations. Anal Biochem 1978;86(1):324–6. https://doi.org/10.1016/0003-2697(78)90350-0. PMid: 655393.
[33] Olasehinde TA, Odjadjare EC, Mabinya LV, et al. *Chlorella sorokiniana* and *Chlorella minutissima* exhibit antioxidant potentials, inhibit cholinesterases and modulate disaggregation of β-amyloid fibrils. Electron J Biotechnol 2019;40:1–9. https://doi.org/10.1016/j.ejbt.2019.03.008.
[34] Nilsson P, Loganathan K, Sekiguchi M, et al. Aβ secretion and plaque formation depend on autophagy. Cell Rep 2013;5(1):61–9. https://doi.org/10.1016/j.celrep.2013.08.042. PMid: 24095740.
[35] Oset-Gasque MJ, Marco-Contelles J. Alzheimer's disease, the "one-molecule, one-target" paradigm, and the multitarget directed ligand approach. ACS Chem Neurosci 2018;9(3):401–3. https://doi.org/10.1021/acschemneuro.8b00069. PMid: 29465220.
[36] Kumari A, Sharma R, Shrivastava N, et al. Bleomycin modulates amyloid aggregation in β-amyloid and hIAPP. RSC Adv 2020;10(43):25929–46. https://doi.org/10.1039/D0RA04949B. PMid: 35518630.
[37] Ashburn TT, Thor KB. Drug repositioning: Identifying and developing new uses for existing drugs. Nat Rev Drug Discov 2004;3(8):673–83. https://doi.org/10.1038/nrd1468. PMid: 15286734.
[38] Bibi N, Rizvi S, Batool A, et al. Inhibitory mechanism of an anticancer drug, bexarotene against amyloid β peptide aggregation: Repurposing via neuroinformatics approach. Curr Pharm Des 2019;25(27):2989–95. https://doi.org/10.2174/1381612825666190801123235. PMid: 31368868.
[39] Breckenridge A, Jacob R. Overcoming the legal and regulatory barriers to drug repurposing. Nat Rev Drug Discov 2019;18(1):1–2. https://doi.org/10.1038/nrd.2018.92. PMid: 29880920.
[40] Oliveira RC, Bandeira PN, Lemos TL, et al. *In silico* and *in vitro* evaluation of efflux pumps inhibition of α, β-amyrin. J Biomol Struct Dyn 2022;40(23):12785–99. https://doi.org/10.1080/07391102.2021.1976277. PMid: 34528866.
[41] Samreen, Qais FA, Ahmad I. *In silico* screening and *in vitro* validation of phytocompounds as multidrug efflux pump inhibitor against *E. coli*. J Biomol Struct Dyn 2023;41(6):2189–201. https://doi.org/10.1080/07391102.2022.2029564. PMid: 35067192.
[42] Panzella L, Eidenberger T, Napolitano A. Anti-amyloid aggregation activity of black sesame pigment: Toward a novel Alzheimer's disease preventive agent. Molecules 2018;23(3):676. https://doi.org/10.3390/molecules23030676. PMid: 29547584.
[43] Meden A, Knez D, Jukič M, et al. Tryptophan-derived butyrylcholinesterase inhibitors as promising leads against Alzheimer's disease. Chem Commun 2019;55(26):3765–8. https://doi.org/10.1039/C9CC01330J. PMid: 30864579.
[44] Pajk S, Knez D, Košak U, et al. Development of potent reversible selective inhibitors of butyrylcholinesterase as fluorescent probes. J Enzyme Inhib Med Chem 2020;35(1):498–505. https://doi.org/10.1080/14756366.2019.1710502. PMid: 31914836.
[45] Aparna V, Dileep KV, Mandal PK, et al. Anti-inflammatory property of *n*-hexadecanoic acid: Structural evidence and kinetic assessment. Chem Biol Drug Des 2012;80(3):434–9. https://doi.org/10.1111/j.1747-0285.2012.01418.x. PMid: 22642495.
[46] Servi H, Sen A, Dogan A. Chemical composition and biological activities of endemic *Tripleurospermum conoclinium* (Boiss. & Balansa) Hayek essential oils. Flavour Fragr J 2020;35(6):713–21. https://doi.org/10.1002/ffj.3610.
[47] do Nascimento KF, Moreira FM, Santos JA, et al. Antioxidant, anti-inflammatory, antiproliferative and antimycobacterial activities of the essential oil of *Psidium guineense* Sw. and spathulenol. J Ethnopharmacol 2018;210:351–8. https://doi.org/10.1016/j.jep.2017.08.030. PMid: 28844678.
[48] Sufriadi E, Meilina H, Munawar AA, et al. Identification of β-Caryophyllene (BCP) in Aceh patchouli essential oil (PEO) using gas chromatography-mass pectrophotometry (GC-MS). InIOP Conf Ser: Earth Environ Sci 2021;667(1):012032. https://doi.org/10.1088/1755-1315/667/1/012032.
[49] Borges F, Roleira F, Milhazes N, et al. Simple coumarins and analogues in medicinal chemistry: Occurrence, synthesis and biological activity. Curr Med Chem 2005;12(8):887–916. https://doi.org/10.2174/0929867053507315.